2015-06

Vertical structure of near-bed cross-shore flow velocities in the swash zone of a dissipative beach

Inch, K

10.1016/j.csr.2015.04.006
Continental Shelf Research
Elsevier BV

Elsevier Editorial System(tm) for Continental Shelf Research
Manuscript Draft

DOI: 10.1016/j.csr.2015.04.006

Title: Vertical structure of near-bed cross-shore flow velocities in the swash zone of a dissipative beach

Article Type: Research Paper

Keywords: swash zone; bed shear stress; friction coefficient; boundary layer; logarithmic model

Corresponding Author: Mr. Kris Inch,

Corresponding Author's Institution: University of Plymouth

First Author: Kris Inch

Order of Authors: Kris Inch; Gerd Masselink; Jack A Puleo; Paul Russell; Daniel C Conley

Abstract: Cross-shore velocity profiles are measured at 0.001 m vertical resolution and at 100 Hz over the lower 0.02 to 0.07 m of the water column in the mid swash zone on a dissipative, macrotidal beach. Swash motion is predominantly at infragravity frequencies and forced by significant wave heights exceeding 1.5 m and peak wave periods over 15 s. Observations of long duration (> 14 s) swashes during two rising tides are used to quantify the vertical structure of cross-shore flow velocities and estimate corresponding bed shear stress and friction coefficients. Analysis is performed on an individual swash event to an elevation of 0.07 m and an ensemble event made up of 24 individual swash events to an elevation of 0.02 m. Cross-shore velocities exceed 2 m s-1 and are of a similar magnitude during both the uprush and the backwash. Changes in velocity with elevation indicate that the swash zone boundary layer extends to 0.07 m during the strongest flows and is well-represented by the logarithmic model applied to this elevation, except near flow reversal. Maximum bed shear stresses estimated using the logarithmic model are 22 N m-2 and 10 N m-2 for the individual event and ensemble event respectively and mean values are larger during the backwash than the uprush. Mean friction coefficients estimated from equating the logarithmic model and the quadratic drag law are 0.018 and 0.019 for the individual event and ensemble event respectively. Bed shear stress may be underestimated if the logarithmic model is fit to a velocity profile that is only part boundary layer, emphasizing the need for high resolution velocity profiles close to the bed for accurate bed shear stress predictions in the swash zone.

Vertical structure of near-bed cross-shore flow velocities in the swash zone of a dissipative beach

Kris Inch[a,*], Gerd Masselink[a], Jack A. Puleo[b], Paul Russell[a] and Daniel C. Conley[a]

[a] *School of Marine Science and Engineering, Plymouth University, Drake Circus, Plymouth, Devon PL4 8AA. United Kingdom.*

kris.inch@plymouth.ac.uk, gerd.masselink@plymouth.ac.uk, P.Russell@plymouth.ac.uk, daniel.conley@plymouth.ac.uk

[b] *Centre for Applied Coastal Research, Department of Civil and Environmental Engineering, University of Delaware, Newark, Delaware 19716.* jpuleo@udel.edu

* Corresponding author. Tel.: +44 (0)1752 586100; Fax: +44 (0)1752 586101; Email: kris.inch@plymouth.ac.uk.

Abstract

Cross-shore velocity profiles are measured at 0.001 m vertical resolution and at 100 Hz over the lower 0.02 to 0.07 m of the water column in the mid swash zone on a dissipative, macrotidal beach. Swash motion is predominantly at infragravity frequencies and forced by significant wave heights exceeding 1.5 m and peak wave periods over 15 s. Observations of long duration (> 14 s) swashes during two rising tides are used to quantify the vertical structure of cross-shore flow velocities and estimate corresponding bed shear stress and friction coefficients. Analysis is performed on an individual swash event to an elevation of

0.07 m and an ensemble event made up of 24 individual swash events to an elevation of 0.02 m. Cross-shore velocities exceed 2 m s^{-1} and are of a similar magnitude during both the uprush and the backwash. Changes in velocity with elevation indicate that the swash zone boundary layer extends to 0.07 m during the strongest flows and is well-represented by the logarithmic model applied to this elevation, except near flow reversal. Maximum bed shear stresses estimated using the logarithmic model are 22 N m^{-2} and 10 N m^{-2} for the individual event and ensemble event respectively and mean values are larger during the backwash than the uprush. Mean friction coefficients estimated from equating the logarithmic model and the quadratic drag law are 0.018 and 0.019 for the individual event and ensemble event respectively. Bed shear stress may be underestimated if the logarithmic model is fit to a velocity profile that is only part boundary layer, emphasizing the need for high resolution velocity profiles close to the bed for accurate bed shear stress predictions in the swash zone.

Keywords: swash zone; bed shear stress; friction coefficient; boundary layer; logarithmic model

1. Introduction

The swash zone is commonly defined as that part of the beach that is alternately covered and exposed by uprush and backwash (Elfrink and Baldock, 2002; Masselink and Puleo, 2006). Large flow velocities in shallow depth, high turbulence levels and large sediment transport rates make the swash zone arguably the most dynamic part of the nearshore region (Masselink *et al.*, 2005; Masselink and Puleo, 2006). These characteristics create sediment transport gradients which drive rapid morphological change on the beachface. Hence, a

detailed understanding of swash zone processes is vital in the modelling of shoreline evolution. The understanding of swash zone processes has progressed considerably over the last decade or so as more specialized sensors have made it easier for coastal scientists to collect data from this notoriously challenging environment. This progress has been documented in a number of review papers (Butt and Russell, 2000; Elfrink and Baldock, 2002; Masselink and Puleo, 2006; Brocchini and Baldock, 2008).

Swash events consist of three distinct phases; uprush, flow reversal, and backwash. A variety of methods have been used to measure the flow characteristics during swash events and several patterns have emerged. Uprush flows typically originate by the collapsing surf zone bore and are sometimes accompanied by a brief period of flow acceleration immediately following bore collapse (Nielsen, 2002; Jensen *et al*., 2003; Puleo *et al*., 2007). The velocity and landward extent of uprush is controlled by the forcing conditions in the surf zone, beach gradient and sediment characteristics. Maximum velocities approaching 2 m s^{-1} have been recorded on gently sloping beaches (Butt and Russell, 1999; Masselink *et al*., 2005) and 3 m s^{-1} on steep beaches (Masselink and Hughes, 1998). Flow velocities are onshore-directed during the uprush, but flow in the lower swash zone often reverses before the uprush has reached its maximum landward extent (Masselink and Puleo, 2006). Backwash flows accelerate under the forces of gravity and offshore-directed pressure gradients (Baldock *et al*., 2001). The duration of backwash is typically longer than that of uprush with slightly weaker velocities (Puleo *et al*., 2003; Masselink *et al*., 2005; Aagaard and Hughes, 2006; Puleo *et al*., 2012).

Several studies have documented the vertical flow structure of swash in laboratory conditions over fixed, impermeable beds. Many of these have fitted cross-shore velocity profiles to a

logarithmic model, commonly known as the Law of Wall, and found excellent agreement ($r^2 >$ 0.9) for most of the swash cycle (Cox *et al*., 2000; Petti and Longo, 2001; Archetti and Brocchini, 2002; O'Donoghue *et al*., 2010; Kikkert *et al*., 2012). This agreement is despite the Law of Wall being designed for steady flows with fully developed boundary layers; not accelerating, reversing or stratified flows. However, fewer studies have attempted to quantify the vertical flow structure of swash on a natural foreshore. This is partially due to instrument limitations that typically do not allow for measurements close to the bed (< 0.02 m), or the deployment of multiple sensors at a particular location. In addition, changes in bed level elevation can occur rapidly under active swash (Masselink *et al*., 2009; Puleo *et al*., 2014a), hence instrument elevation will vary during a swash event, over a tidal cycle and indeed throughout a field experiment. Raubenheimer *et al*. (2004) used acoustic Doppler velocimeters (ADV) to obtain velocities at elevations of 0.02, 0.05 and 0.08 m above the bed on a gently sloping beach. The cross-shore velocity profiles were fitted to the logarithmic model and were found to be approximately logarithmic within 0.05 m of the bed. Masselink *et al*. (2005) recorded the velocity at 0.03 and 0.06 m above the bed using electromagnetic current meters and reported that the thickness of the boundary layer was at least 0.03 m during the start and end of the swash cycle on a low gradient, macrotidal beach. More recently, using a newly developed high resolution acoustic Doppler current profiler, Puleo *et al*. (2012) measured the cross-shore velocity profile in the lower 0.02 m of the water column at a spatial resolution of 0.001 m on a microtidal, low energy beach. Cross-shore velocities in the lower 0.02 m of the water column were well represented by the logarithmic model ($r^2 >$ 0.9), except around the time of flow reversal. Despite being undertaken on a natural beach, the energy level of the forcing conditions during this study is comparable to that observed under laboratory settings with significant wave heights not exceeding 0.16 m and peak wave periods between 4 and 6 s. Instrument limitations have required that past studies assume that

the logarithmic boundary layer is at least as large as the elevation of the highest sensor used in applying the logarithmic model. More research is needed to explore how the model applicability is influenced by the number of points used in the velocity profile and the elevation over which the Law of Wall is applied.

A number of previous studies have estimated bed shear stress in the swash zone indirectly using the Law of Wall or the quadratic drag law. A considerable variation of bed shear stress estimates in the swash zone exists in the literature. This variation can be attributed partly to differences in estimation techniques, forcing conditions and the cross-shore location in the swash zone where measurements were taken. A general trend in both laboratory (Archetti and Brocchini, 2002; Cowen *et al*., 2003; Kikkert *et al*., 2012) and field studies (Masselink *et al*., 2005) is for bed shear stress to be larger during uprush than backwash. For example, Masselink *et al*. (2005) calculated maximum bed shear stresses during the uprush of around 25 N m^{-2} and only 10 N m^{-2} during backwash on a dissipative beach with a significant wave height of 1.5 m. This trend is consistent with direct measurements of bed shear stress made in the laboratory (Barnes *et al*., 2009) and the field (Conley and Griffin, 2004). Direct measurements of bed shear stress taken by Conley and Griffin (2004) using a flush mounted hot film anemometer were, however, an order of magnitude smaller than those estimated by Masselink *et al*. (2005). The difference between uprush and backwash shear stress magnitudes is generally attributed to excessive bore-related turbulence during the uprush and, in the field, the thinning of the boundary layer due to infiltration (Conley and Inman, 1994; Petti and Longo, 2001). In contrast to this trend, Puleo *et al*. (2012) calculated peak bed shear stresses of 4 N m^{-2} during uprush and 7 N m^{-2} during backwash using high resolution velocity profiles measured during low energy conditions. However, due to the use of acoustic sensors in this study, the velocity profile at the beginning of the uprush when bed shear stresses are

potentially largest was not measured. Additionally, Puleo *et al*. (2012) estimated bed shear stress using cross-shore velocities from only two elevations above the bed, analogous to the method used by Masselink *et al*. (2005). Differences of nearly 100% were reported between the two methods, suggesting that more highly resolved cross-shore velocity profiles are necessary to give an accurate estimate of bed shear stress using the logarithmic model.

The quadratic drag law has been widely used to calculate bed shear stress when velocity profile information is not available. This method is dependent upon a free stream velocity measurement and a friction coefficient which is normally a constant value. Several studies have inferred swash zone friction coefficients by equating the logarithmic model and the quadratic drag law when profile data exist. Results from these studies vary significantly ($0.001 < f < 1$) (Cox *et al*., 2000; Archetti and Brocchini, 2002; Cowen *et al*., 2003; Raubenheimer *et al*., 2004; Barnes *et al*., 2009; O'Donoghue *et al*., 2010; Puleo *et al*., 2012). This variance is due mostly to differences in experimental conditions. In studies where bed shear stress was larger (smaller) during uprush, the mean friction coefficient during uprush was also greater (lesser) (Archetti and Brocchini, 2002; Cowen *et al*., 2003; Puleo *et al*., 2012). Friction coefficients estimated at different locations in the swash zone of a laboratory beach were relatively constant across the full width of the swash zone (Barnes *et al*., 2009). The friction coefficient is heavily influenced by the elevation above the bed at which the velocity used in the quadratic drag law is obtained. This velocity is usually taken from the highest current meter without knowledge of whether or not the velocity is located in the free stream. Puleo *et al*. (2012) explored the impact of using velocities from different elevations and found that the friction coefficient is considerably larger when velocities close to the bed are used. For example, using the velocity from an elevation of 0.02 m gave a mean friction

coefficient of 0.034, whereas the velocity from 0.005 m gave a mean friction coefficient of 0.11.

Past studies have indicated that the logarithmic model may be applicable to swash flow, except during the initial stages of uprush and during flow reversal. However, the model is yet to be fully validated with high resolution velocity profile measurements under high energy conditions on a natural foreshore. Evidence suggests that high resolution velocity profiles close to the bed are necessary for improving confidence in estimating swash zone bed shear stresses and sediment transport rates. This paper reports on high resolution (0.001 m) cross-shore velocity profiles that have been recorded in the swash zone boundary layer of a high energy, dissipative beach. The main objectives of this paper are to: (1) investigate the applicability of the logarithmic model; (2) to identify temporal variability in the thickness of the swash zone boundary layer; and (3) to quantify corresponding bed shear stresses and friction coefficients.

2. Methodology

2.1. Field site and data collection

The BeST (Beach Sand Transport) field experiment was conducted from 9 to 15 October 2011 on Perranporth Beach, Cornwall, England (Fig. 1) with the purpose of collecting a comprehensive dataset of swash zone hydrodynamics and sediment transport (see Puleo *et al.*, 2014b; for an extensive description of the BeST field experiment). Perranporth is a macrotidal, dissipative beach with a mean tidal range of 5.43 m. The beach faces west-

northwest and is exposed to both Atlantic swell and locally generated wind waves. The beach is approximately 3.5 km long and is enclosed by two headlands; Ligger Point to the north and Droskyn Point to the south. The nearshore is characterised by a low-gradient, concave profile composed of medium sand with a median grain size D_{50} of 0.33 mm during the field experiment.

Data collected during two high tides on 12 and 13 October are discussed in this paper. These tides were chosen as the data contained good velocity profile coverage during moderate forcing conditions. Offshore wave conditions, measured by a Datawell Directional Waverider buoy in approximately 10 m water depth (see Fig. 1), were similar during both tides with significant wave heights of 1.55 m and 1.47 m, and peak wave periods of 15.4 s and 13.0 s, respectively (Fig. 2). Offshore wave direction varied with tidal phase; however, waves in the surf and swash zones were relatively shore-normal (Puleo *et al*., 2014b). The beach slope near mean high water steepened slightly from 0.0245 (1:41) to 0.0251 (1:40) over the two high tides, as might be expected from the arrival of long period swell waves.

A range of instruments were mounted onto a 45 m long scaffold rig erected near the high tide line, with a main instrument bar situated 7.4 m for the rig's seaward edge near the mean high water line (Fig. 3). Puleo *et al*. (2014b) provides a detailed description of the instrument deployment. This paper predominantly uses high resolution near-bed velocity data recorded by 3 Nortek Vectrino II acoustic Doppler current profilers mounted onto the main instrument bar. Each Vectrino II records the velocity profile (*u*,*v*,*w*) over a range of 0.03 m at 0.001 m vertical bin spacing and at a sampling frequency of 100 Hz. The lowest Vectrino II was initially arranged so that the lower 0.01 m of the profiling range was located within the bed at the start of each high tide. The two additional Vectrino IIs were situated at 0.025 m vertical

offsets and 0.2 m alongshore offsets. This arrangement allowed the velocity profile to be recorded to an elevation of around 0.07 m above the bed at 0.001 m spacing.

Vertical adjustments were made following each tide, as necessary, to return the sensors to their intended elevations. An ultrasonic bed-level sensor (BLS) (Turner *et al*., 2008) located adjacent to the Vectrino II sensors was used to measure the water depth at a sampling frequency of 4 Hz. All instruments were referenced to a local coordinate system and cabled to shore where data were recorded on a bank of computers that were time synchronised to a GPS clock (UTC).

2.2. Data analysis

2.2.1. Data quality control, event selection and ensemble-averaging

Vectrino II data were removed from the record if the beam correlations were less than 60% or the amplitude of 2 or more beams was less than -30 dB (Puleo *et al*., 2012; Puleo *et al*., 2014b). This process removes unreliable data most commonly associated with foam/bubbles or a large sediment load. The Vectrino II time series was despiked by removing data where the velocity difference between two subsequent measurements was > 0.5 m s^{-1}, synonymous with a clearly inaccurate flow acceleration of 50 m s^{-2}.

The intermittent nature of swash precludes the application of conventional time series analysis. As a result, the vast majority of studies base their analysis on the identification of individual swash 'events'. A common problem encountered when studying swash is how to define and select these events. Turbulence at the start of the uprush can lead to velocity data being removed in quality control procedures, while the backwash phase becomes truncated

when the water elevation becomes less than that of the current meter. The BLS on the main instrument bar is used to identify swash events overcoming the limitation based on elevated current meters. A swash event is defined as beginning when the water depth rises above zero and ending when the water depth returns to zero. The water depth during swash flow is quantified by subtracting the most recent bed elevation from the BLS data when the bed was exposed (Turner *et al*., 2008). The bed location is identified as being the highest bin from the lowest Vectrino II sensor where the mean velocity and standard deviation are both less than 0.05 m s^{-1} (Puleo *et al*., 2012; Puleo *et al*., 2014b). This value was checked by visual inspection and data from below the bed were discarded. The bed level is assumed to remain constant over the duration of an event. The majority of events identified for analysis come from within the first hour of the sampling period of each tide when the main instrument bar was located in the mid swash zone. We focus on data from the rising tide because the bed level lowered throughout each tide beyond the range of the lowest sensor, thus making the bed location unidentifiable during the falling tide. It is important to be aware of the tidal stage when interpreting the results as the characteristics of swash flow in the mid swash zone are not always representative of swash flows further seaward (Masselink and Puleo, 2006). The conditions under which the data were collected are characterised in Fig. 4 which shows a sample of the BLS data from the high tide sampling period on 12 October.

Combining data from the three Vectrino II sensors proved to be problematic as the 0.2 m alongshore separation of the sensors caused significant hydrodynamic variability. Therefore, to minimise possible error, only data from the lowest sensor are used to create an ensemble-averaged swash event. Only events that meet the following criteria were included in the ensemble-averaging: (1) total event duration is greater than 14 s; (2) uprush and backwash phase duration are each greater than 5 s; (3) the bed location is identifiable; and (4) maximum

uprush and backwash velocities exceed 1 m s^{-1} in the top bin of the lowest sensor. Events that meet these criteria were normalised by their duration to a non-dimensional time scale t/T, where t is time and T is event duration (Puleo *et al*., 2003; Conley and Griffin, 2004; Masselink *et al*., 2005; Aagaard and Hughes, 2006; Barnes *et al*., 2009; Puleo, 2009). The events were then combined into an ensemble-averaged event representing mean flow patterns. A total of 24 events were used in the ensemble-averaging (Table 1). Mean duration ± 1 standard deviation of the events used in the ensemble-averaging is 17.58 ± 2.77 s.

Table 1. Summary statistics of the swash events used in the ensemble-averaging. The error associated with the maximum velocities from the Vectrino II, according to the manufacturer, are expected to be no more than ± 0.5% of the measured value ± 1 mm s^{-1}. Event No. 23 (shaded) is the individual event used in the analysis.

$No.$	D (s)	D_u (s)	D_b (s)	$\hat{u}_u$ (m s^{-1})	$\hat{u}_b$ (m s^{-1})
Swash events measured on 12/10/2011					
1	14.46	6.26	8.20	1.53	1.48
2	18.36	7.49	10.87	1.08	1.15
3	17.07	6.00	11.07	1.30	1.20
4	24.52	9.45	15.07	1.14	1.80
5	20.50	7.06	13.44	1.29	1.22
6	15.16	5.26	9.90	1.26	1.38
7	17.01	6.62	10.39	1.16	1.30
8	18.61	6.66	11.95	1.58	1.49
9	16.21	7.27	8.94	1.13	1.06
10	15.66	6.82	8.84	1.56	1.16
11	18.12	6.39	11.73	1.76	1.48
12	21.35	9.71	11.64	2.00	1.95
13	23.64	11.84	11.80	1.89	1.62
14	19.20	9.01	10.19	1.37	1.31

Swash events measured on 13/10/2011

15	15.08	5.85	9.23	1.32	1.37
16	16.81	6.54	10.27	1.28	1.19
17	17.75	6.89	10.86	1.70	1.41
18	16.89	5.88	11.01	1.57	1.78
19	14.28	4.93	9.35	1.37	1.22
20	15.83	6.52	9.31	1.32	1.20
21	14.89	6.85	8.04	1.39	1.56
22	14.76	5.69	9.07	1.24	1.42
23	18.22	7.68	10.54	2.14	1.88
24	16.08	7.13	8.95	1.72	1.68
Mean	17.52	7.08	10.44	1.46	1.43
StDev	2.74	1.56	1.65	0.29	0.25

D = total duration, D_u = uprush duration, D_b = backwash duration, $\hat{u}_u$ = maximum velocity during uprush, $\hat{u}_b$ = maximum velocity during backwash.

2.2.2. Logarithmic velocity profile and bed shear stress

The von Karman-Prandtl relationship is used to quantify the logarithmic shape of the velocity profile within a fully developed boundary layer as

$$u(z) = \frac{u_*}{\kappa} ln\left(\frac{z}{z_0}\right) \qquad (1)$$

where $u(z)$ is the cross-shore velocity profile, κ is von Karman's constant (0.4), z_0 is the roughness height and u_* is the shear velocity. Theoretically the logarithmic model is valid when $30 < z^+ < 1200$, where z^+ is the non-dimensional elevation defined as $z^+ = \frac{u_* z}{\nu}$ and ν is the kinematic viscosity (Wei and Willmarth, 1989; Pope, 2000). A least squares regression is performed between the velocity profile (u) and $ln(z)$. The square of the correlation coefficient in the regression is used to accept or reject the logarithmic model and the slope m

of the least squares regression is used to infer the shear velocity by $u_* = m\kappa$ and the bed shear stress through

$$u_* = \sqrt{\tau/\rho} \qquad (2)$$

where τ is the bed shear stress and ρ is the water density. When velocity profile information is not available, the bed shear stress is estimated by the quadratic drag law as

$$\tau = 0.5\rho f u_f |u_f| \qquad (3)$$

where f is a friction coefficient, u_f is the free stream velocity and | | indicate absolute value (to maintain relative flow direction). When velocity profile data are available, the friction coefficient is estimated using Eqs. (2) and (3) as

$$f = \frac{2u_*|u_*|}{u_f|u_f|} \qquad (4)$$

Eqs. (1)-(4) were applied to an individual swash event to an elevation of 0.07 m and to an elevation of 0.02 m for the ensemble-averaged event. The individual swash event (No. 23 in Table 1) was chosen due to the consistent transition between data from the three Vectrino II sensors for the duration of the event. This was not generally the case for all events so the ensemble was taken to an elevation of 0.02 m only.

3. Results

3.1 Description of swash events

The time series of swash depth and flow velocity for the individual swash event and ensemble swash event are shown in Fig. 5. Both events show a rapid increase in swash depth at the start of the uprush as the flows reach the main instrument bar. During the individual event, swash depth reaches its maximum early in the uprush and decreases steadily throughout the rest of the event. Similarly, the ensemble swash depth is at its maximum during the uprush, but remains relatively constant until just before flow reversal and then decreases during the backwash. Both events have a longer backwash phase with flow reversal occurring around 7.7 s into the individual event (total duration = 18.2 s), and at a normalised time of t/T = 0.4 during the ensemble event. This is typical of skewed swash motion on a dissipative beach (Masselink and Puleo, 2006).

For clarity, only velocities from several bin elevations are plotted in Fig. 5C-D. Velocity magnitudes exceed 2 m s^{-1} during the individual event, with maximum uprush velocities exceeding those in the backwash. Maximum velocities during the ensemble event are similar during uprush and backwash but do not exceed 1.5 m s^{-1}, attributable to only the lowest sensor being used in the ensemble-averaging. Vertical velocity variations are assumed to result solely from friction at the bed and thus the vertical extent of these variations is termed the boundary layer. Boundary layer thickness varies with flow phase, as identified by the vertical separation of the velocity time series in Fig. 5C-D. For example, near the beginning of the uprush in the ensemble event (t/T = 0.1) there is sequential vertical separation between all of the time series indicating that the boundary layer must be at least 0.02 m thick as flow velocity is increasing vertically to at least this elevation. Later in the uprush at t/T =

0.3, the boundary layer thickness is reduced as evidenced by the small vertical separation between individual velocity time series from elevations higher than 0.006 m above the bed. At flow reversal (t/T = 0.4), there is almost no separation between the different time series as the boundary layer is virtually non-existent. The boundary layer grows during the backwash and is at least 0.02 m thick by t/T = 0.9 as depicted by clear vertical separation of all of the time series.

3.2 Logarithmic model

An r^2 cut-off of 0.9 is used for the ensemble-averaged event, below which the logarithmic model fit is considered poor. This cut-off has been adopted by the majority of previous studies that have completed similar analyses (e.g., O'Donoghue *et al*., 2010; Puleo *et al*., 2012) and allows for a direct comparison with the results of these studies. However, an r^2 value this high is not appropriate where ensemble-averaging has not been performed and velocity fluctuations are abundant. Therefore, an r^2 cut-off of 0.8 is used to indicate poor model fit for the individual swash event. Additionally, the velocity time series of the individual event is block averaged over 0.1 s (10 measurements) to smooth out some of these fluctuations. All r^2 values reported here are significant at the 95% level.

The logarithmic model describes accurately the velocity profile of the individual swash event with r^2 exceeding 0.8 for 63% of its duration (Fig. 6A-D). The uprush in particular is well described by the logarithmic model applied to 0.07 m above the bed. The model fit becomes poor just prior to flow reversal and r^2 remains below 0.8 for almost half of the backwash before improving. It must be noted that missing measurements at the start and end of the event, as a result of quality control procedures discarding turbulent data and the water depth

being below that of the upper most bin, prevent the application of the logarithmic model. Error between the logarithmic model and the data is generally low (mean = 11.9%), except close to the bed where it exceeds 50% at times, particularly during the uprush. Estimates of z_0 from the logarithmic model fits yield 0.0008 ± 0.0005 m (mean ± standard deviation).

The ensemble event is generally well described by the logarithmic model with r^2 exceeding 0.9 for 66% of the event (Fig. 6E-H). As with the individual event, poor model fit occurs at the end of the uprush, at flow reversal, and for a significant time at the beginning of the backwash. Mean error between the data and the logarithmic model is less than the individual event at 8.4%, owing to the smoothing of turbulent fluctuations in the ensemble-averaging procedure. However, error can still exceed 50% close to the bed. As with the individual event, mean z_0 is less than the elevation of the bottom profiling bin at 0.0003 ± 0.0002 m. Values of z_0 are similar during the uprush and backwash and increase slightly close to flow reversal.

Fig. 7C-D shows example velocity profiles from eight evenly spaced times during the individual and ensemble swash events, identified by the coloured dots in Fig. 7A-B. Logarithmic model fits are also shown (solid lines) if $r^2 > 0.8$ or 0.9 for the individual and ensemble swash events, respectively. The model is fit to the velocity profile at 0.001 m resolution; however, for clarity the velocity profiles in the individual swash event are plotted at 0.003 m resolution. All of the example velocity profiles in the individual swash event have clear curvature with smaller velocities near the bed representing the presence of a boundary layer, with the exception of the velocity profile occurring at flow reversal (turquoise dots). Boundary layer decay during the uprush and growth during the backwash is evident from the velocity profiles. For example, the velocity profile from early in the backwash (yellow dots) appears to have a boundary layer thickness of about 0.02 m, above which the velocity

remains at around 0.6 m s^{-1}. The velocity profile from approximately 7 s later (orange dots), where the velocity exceeds 1.5 m s^{-1} in the upper bins, indicates that the boundary layer extends to the top of the profile at 0.07 m.

In the ensemble swash event, the logarithmic model (solid curves) is applicable (r^2 > 0.9) for all of the example velocity profiles except the three closest to flow reversal. The shape of the velocity profiles indicate that the boundary layer thickness is at least 0.02 m during the strongest flows (red, gray and orange velocity profiles), but less when velocities are weaker (< 0.5 m s^{-1}) allowing the profile to become more depth-uniform.

3.3 Bed shear stress and friction coefficients

Bed shear stress estimates from fitting the logarithmic model to the velocity profile vary between 0 and 22 N m^{-2} for the individual swash event (Fig. 8A), and 0 and 10 N m^{-2} for the ensemble swash event (Fig. 8B). Mean bed shear stresses during the uprush are less than those during the backwash: 6 N m^{-2} and 8 N m^{-2} for the individual event; and 3 N m^{-2} and 6 N m^{-2} for the ensemble event. Bed shear stresses decrease towards zero during the uprush and increase during the backwash. Where the logarithmic model fit was less than the correlation cut-off, bed shear stress was not quantified. Due to the high r^2 cut-off and the large number of measurements in the velocity profile, the error associated with the logarithmic model fit is low with mean bed shear stress errors for the individual and ensemble events equating to 0.019 N m^{-2} and 0.07 N m^{-2} respectively.

When velocity profile data are not available, past studies have used the quadratic drag law (Eq. (3)) with a constant friction coefficient to estimate bed shear stress. A comparison

between bed shear stress estimates using the logarithmic model and the quadratic drag law is presented for the individual and ensemble swash events (Fig. 8A-B). Using a constant friction coefficient of 0.012, based on the Swart (1974) formula, quadratic drag law estimates of bed shear stress follow the same general trend as those from the logarithmic model with values decreasing during the uprush and increasing during the backwash. Mean bed shear stress using the quadratic drag law is 6 N m^{-2} and 4 N m^{-2} for the individual and ensemble events respectively, compared to 7 N m^{-2} and 5 N m^{-2} if the logarithmic model is used. This difference is best seen in the latter stages of the uprush and middle stages of the backwash for the ensemble event, corresponding to when the friction coefficients estimated from the logarithmic model become significantly larger than those used in the quadratic drag law. However, given the spread in the estimates, particularly for the individual event, and the strong sensitivity of the quadratic drag law to changes in u_f, the small difference in bed shear stress estimates between the logarithmic model and the quadratic drag law cannot be considered significant. For example, when a constant friction coefficient of 0.012 is used with the quadratic drag law, bed shear stress will increase from 6 N m^{-2} to 7 N m^{-2} with a velocity increase of < 0.1 m s^{-1}.

In estimating the friction coefficient f (Eq. (4)), u_f is taken from an elevation of 0.07 m for the individual swash event and 0.02 m for the ensemble swash event. Friction coefficients are 0.018 ± 0.008 and 0.019 ± 0.007 (mean ± standard deviation) for the individual and ensemble swash events respectively (Fig. 8C-D). Owing to the turbulent nature of the individual event, estimates of f show considerable variability without any obvious trends. The ensemble swash event shows a more systematic trend in f with values increasing during the uprush to a maximum just before flow reversal, and decreasing during the backwash. Mean f values during the uprush and backwash are of a similar magnitude. Mean error associated with the

friction coefficients is < 3% of the estimated value for both the individual and ensemble swash events.

4. Discussion

4.1 Velocity profiles and the logarithmic model

The velocities measured in this study are comparable to those reported by Butt and Russell (1999) and Masselink *et al*. (2005) under similar forcing conditions at the same beach. The velocity data suggest that the boundary layer thickness is at least 0.07 m during the strongest flows, similar to results inferred by Raubenheimer *et al*. (2004) and Masselink *et al*. (2005) on dissipative beaches. It is important to highlight that the data used in this study were collected from a single location, whereas boundary layer structure varies with location in the swash zone as well as with time. At the seaward end of the swash zone, the velocity profile at the beginning of the uprush can be nearly depth-uniform as turbulence from bore collapse acts to homogenize the water column (Puleo *et al*., 2000; Petti and Longo, 2001; Cowen *et al*., 2003). The data used in this study came from the beginning of the two high tides when the main instrument bar would have been located in the mid part of the swash zone. This suggests that most of the bore turbulence would have dissipated and the uprush boundary layer would have had time to mature as the swash lens climbed the beach, especially considering the large swash excursion typical of infragravity swash motion. This could explain the well-developed boundary layer and success of the logarithmic model for the majority of the uprush. Given the location of the sensors in the mid swash zone when data were collected, the backwash boundary layer is relatively young and therefore likely to be

thinner than the boundary layer would have been further seaward in the swash zone. Yet the boundary layer still extends to at least 0.07 m during the strongest flows, suggesting that the boundary layer thickness could become considerably larger than this.

The logarithmic model describes well the cross-shore velocity profile in both the individual and ensemble swash events, except when velocities are particularly low and the boundary layer is thin or non-existent. These results are in agreement with most previous studies that have applied the logarithmic model (e.g., Cox *et al*., 2000; Raubenheimer *et al*., 2004; O'Donoghue *et al*., 2010; Puleo *et al*., 2012). Past studies have applied the logarithmic model to the available data from fixed current sensors and if r^2 between the velocity profile and the model exceeds a particular value (normally 0.9 for ensemble-averaged swash events) then that profile up to the elevation of the highest sensor is assumed to be logarithmic. However, in a test of the sensitivity of r^2 which involved fitting u_f measurements to a logarithmic velocity profile (r^2 = 1) of varying heights, it was found that the number of u_f measurements required for r^2 to become less than 0.9 is ~1.5 times the number of measurements in the logarithmic profile (i.e., fitting the logarithmic model to a 0.02 m thick logarithmic boundary layer and a 0.03 m free stream layer yielded an r^2 of ~0.9). Although field data are unlikely to ever be perfectly logarithmic, this has important implications when applying the logarithmic model to elevations farther from the bed and may have a significant impact on the parameters obtained from the model, especially when the presence of a transitional, outer (non-logarithmic) boundary layer is considered.

Furthermore, it was assumed that the bed level remained constant throughout the swash events. However, the results of Lanckriet *et al*. (2014) and Puleo *et al*. (2014a) using data collected by conductivity concentration profilers (CCP) during the BeST field experiment

indicate that this assumption may not be valid. Precise knowledge of sensor elevation above the bed is important for accurately determining estimates of bed shear stress and friction coefficients. For example, Raubenheimer *et al*. (2004) states that a ± 0.01 m error in sensor elevation can lead to friction coefficients being over or underestimated by 40%.

A significant problem encountered during this study was that of combining data from the three Vectrino II sensors. Initial intentions were to have measurements up to an elevation of 0.07 m for all swash events analysed; however, this was not possible due to variations caused by the alongshore separation of sensors and possibly longshore velocities that frequently exceeded 1 m s^{-1} induced by oblique swash motion. It is most likely that this has impacted the data in past studies that have used sensors in an alongshore arrangement, but only now that there is some overlap between the measurements has it become evident. Until a single sensor is developed with a larger profiling range, this will continue to be an issue when multiple sensors are used.

4.2 Bed shear stress

Based on the sensitivity of r^2 to u_f measurements discussed in section 4.1, Fig. 9 shows the effect of estimating bed shear stress from the logarithmic model fit to different maximum elevations in the velocity profile, whilst always including the lower 0.05 m. While the temporal trend in bed shear stress with swash phase remains the same, mean values increase as upper sections of the velocity profile are removed from the model fit. This is most apparent during the middle stages of the backwash in both the individual and ensemble events. For example, mean bed shear stress between t/T = 0.5-0.8 in the ensemble event is 5.2 N m^{-2} if the whole 0.02 m of the velocity profile is used in the model fit, but 6.6 N m^{-2} if only the

lower 0.015 m of the velocity profile is used and 7.8 N m^{-2} if only the lower 0.005 m of the velocity profile is used. This is because the lower portion of the velocity profile, where the vertical change in velocity is greater, is being better resolved by the logarithmic model. Fitting the logarithmic model to the whole velocity profile when it consists largely of free stream velocities or velocities in the outer boundary layer acts to reduce the slope of the model fit, thus producing lower shear velocities and bed shear stress estimates. Estimates of bed shear stress at the beginning of the uprush and end of the backwash, when the boundary layer is more developed and extends to the top of the velocity profile (Fig. 7C-D), are similar regardless of the maximum elevation used in the logarithmic model. These findings suggest that it is not always appropriate to fit the logarithmic model to all available measurements and that high resolution velocity profiles that include measurements in close proximity (< 0.01 m) to the bed are required to identify the boundary layer region and obtain reliable bed shear stress estimates.

Peak bed shear stresses are larger than those reported in the field by Conley and Griffin (2004) and Puleo *et al*. (2012) under less energetic forcing conditions, but similar to those estimated by Masselink *et al*. (2005) under comparable forcing conditions. The trend of higher bed shear stresses during the backwash than the uprush is in contrast with many past field studies (Cox *et al*., 2000; Archetti and Brocchini, 2002; Cowen *et al*., 2003; Conley and Griffin, 2004; Masselink *et al*., 2005; Barnes *et al*., 2009; Kikkert *et al*., 2012), but in agreement with Puleo *et al*. (2012) where high resolution data from a Vectrino II sensor were also used. It must be acknowledged that the true peak bed shear stress during the uprush may be larger than those calculated but is potentially undetermined due to velocity data from the beginning of the uprush being removed in the quality control procedure. Higher bed shear stresses during the uprush are normally attributed to bore-generated turbulence impinging on the bed

(Puleo *et al*., 2000). However, Osborne and Rooker (1999) investigated turbulent energy in the swash zone and concluded that the influence of bore turbulence is short lived following bore collapse. Therefore, turbulence is likely to have been less significant in this study due to the distance between bore collapse and the location of the instruments. Additionally, the short period of flow acceleration at the beginning of the uprush responsible for enhancing bed shear stress in some studies is also absent from the data record. These factors suggest that the bed shear stresses presented may not be representative of flows further seaward in the swash zone. Higher bed shear stresses at the beginning of the uprush and end of the backwash are to be expected because of the higher flow velocities and steeper velocity gradient at these times.

4.3 Friction coefficient

Mean friction coefficients in this study are similar during uprush and backwash, as has been reported by some previous studies (Raubenheimer *et al*., 2004; Masselink *et al*., 2005; Kikkert *et al*., 2012). However, this contradicts several studies that have found uprush friction coefficients to exceed those during the backwash (e.g., Cox *et al*., 2000; Archetti and Brocchini, 2002; Cowen *et al*., 2003; Conley and Griffin, 2004). While there is no general explanation for larger friction coefficients during uprush, it has often been related to bore turbulence which, as argued previously, is unlikely to have had a significant impact on the data in this study. Friction coefficients estimated in this study, particularly for the ensemble swash event, show an increase during the uprush and a decrease during the backwash, with maximum values occurring close to flow reversal. Few studies have reported this trend, although Barnes *et al*. (2009) and Kikkert *et al*. (2012) suggest that it is consistent with behaviour in uniform, steady flows in that the friction coefficient is increasing with decreasing Reynolds number and higher relative roughness, and vice versa during the

backwash. Barnes *et al*. (2009) reported friction coefficients in a laboratory experiment trending towards infinity at flow reversal when the free stream velocity and Reynolds number approach zero. Friction coefficients in the present study may also follow this trend but could not be calculated at flow reversal due to poor fit of the logarithmic model. Barnes *et al*. (2009) also propose that friction coefficients, despite being time-varying, are more spatially constant than bed shear stress. This would suggest that, despite the data in this study being collected from the mid swash zone, the general trend observed between uprush and backwash friction coefficients may also be representative of flow further seaward in the swash zone.

A potential source of error when estimating the friction coefficient stems from the use of u_f. Friction coefficient estimates will always be erroneous if u_f is taken from within the boundary layer. An investigation into the use of u_f from different elevations in the boundary layer (not shown) shows that friction coefficients are increasingly overestimated as velocities closer to the bed are used. This is similar to the findings of Puleo *et al*. (2012) who also investigated u_f elevation but only within 0.02 m of the bed. The velocity profiles in this study indicate that the boundary layer is at least 0.07 m during the strongest flows. This suggests that at least some of the friction coefficient estimates for the individual event may have been overestimated, and a larger portion for the ensemble event where u_f was taken from 0.02 m.

5. Conclusions

High resolution (0.001 m) cross-shore velocity profiles measured under energetic forcing conditions on a natural foreshore are presented. Velocity profiles indicate that the total height of the boundary layer exceeds 0.07 m at the beginning of the uprush and end of the backwash

when flow velocities are largest. The logarithmic model describes well the velocity profile up to an elevation of 0.07 m above the bed and maximum bed shear stress inferred from the logarithmic model fit to this elevation is 22 N m^{-2}. This is consistent with estimates from previous studies with similar forcing conditions. Unlike many past studies, however, mean bed shear stresses during the backwash are higher than those during the uprush. This can partially be attributed to the data being collected from the mid swash zone and may be impacted by the selection criteria. Temporal variation of the friction coefficient is observed, but mean values are similar for the uprush and backwash at around 0.018. High resolution measurements from across the swash zone are needed to address the importance of swash location on the findings reported herein. Estimates of bed shear stress may be underestimated if the logarithmic model is applied to a velocity profile that is not entirely within the boundary layer. This accentuates the need for highly resolved velocity measurements in close proximity to the bed for accurate estimates of bed shear stress, and thus sediment transport predictions.

Acknowledgements

The BeST field experiment was supported by the National Environmental Research Council (Grant NE/G007543/1), an Australian Research Council Discovery Project (DP110101176), and the US-UK Fullbright Commission. Additional support was provided by the National Science Foundation (Grant No. OCE-0845004 and OCE-1332703) and the University of Delaware. The authors would like to thank D. Buscombe, C. Blenkinsopp, P. Ganderton, A. Jane, L. Joia, T. Lanckriet, R. McCall, A. McIver, L. Melo De Almeida, T. Poate, B. Pronenca, C. Rosario, M. Sheridan and I. Turner for their assistance in the field

measurements. The comments and suggestions of two anonymous reviewers greatly improved the manuscript.

References

Aagaard, T., Hughes, M.G., 2006. Sediment suspension and turbulence in the swash zone of dissipative beaches. Mar. Geol. 228, 117-135. http://dx.doi.org/10.1016/j.margeo.2006.01.003.

Archetti, R., Brocchini, M., 2002. An integral swash zone model with friction: an experimental and numerical investigation. Coast. Eng. 45, 89-110. http://dx.doi.org/10.1016/S0378-3839(02)00038-8.

Baldock, T.E., Baird, A.J., Horn, D.P., Mason, T., 2001. Measurements and modelling of swash-induced pressure gradients in the surface layers of a sand beach. J. Geophys. Res. 106, 2653-2666. http://dx.doi.org/10.1029/1999JC000170.

Barnes, M.P., O'Donoghue, T., Alsina, J.M., Baldock, T.E., 2009. Direct bed shear stress measurements in bore-driven swash. Coast. Eng. 56, 853-867. http://dx.doi.org/10.1016/j.coastaleng.2009.04.004.

Brocchini, M., Baldock, T.E., 2008. Recent advances in modelling swash zone dynamics: Influence of surf-swash interaction on nearshore hydrodynamics and morphodynamics. Rev. Geophys. 46, RG3003. http://dx.doi.org/10.1029/2006RG000215.

Butt, T., Russell, P., 1999. Suspended sediment transport mechanisms in high-energy swash. Mar. Geol. 161, 361-375. http://dx.doi.org/10.1016/S0025-3227(99)00043-2.

Butt, T., Russell, P., 2000. Hydrodynamics and Cross-Shore Sediment Transport in the Swash-Zone of Natural Beaches: A Review. J. Coast. Res. 16, 255-268. http://www.jstor.org/stable/4300034.

Conley, D.C., Inman, D.L., 1994. Ventilated oscillatory boundary layers. J. Fluid Mech. 273, 261-284. http://dx.doi.org/10.1017/S002211209400193X.

Conley, D.C., Griffin, J.G., 2004. Direct measurements of bed stress under swash in the field. J. Geophys. Res. 109, C03050. http://dx.doi.org/10.1029/2003JC001899.

Cowen, E.A., Sou, I.M., Liu, P.L.F., Raubenheimer, B., 2003. Particle Image Velocimetry Measurements within a Laboratory-Generated Swash Zone. J. Eng. Mech. 129, 1119-1129. http://dx.doi.org/10.1061/(ASCE)0733-9399(2003)129:10(1119).

Cox, D.T., Hobensack, W.A., Sukumaran, A., 2000. Bottom Stress in the Inner Surf and Swash Zone. Proceedings of the 27th International Conference on Coastal Engineering, ASCE. pp. 108-109. http://dx.doi.org/10.1061/40549(276)9.

Elfrink, B., Baldock, T., 2002. Hydrodynamics and sediment transport in the swash zone: a review and perspectives. Coast. Eng. 45, 149-167. http://dx.doi.org/10.1016/S0378-3839(02)00032-7.

Jensen, A., Pedersen, G.K., Wood, D.J., 2003. An experimental study of wave run-up at a steep beach. J. Fluid Mech. 486, 161-188. http://dx.doi.org/10.1017/S0022112003004543.

Kikkert, G.A., O'Donoghue, T., Pokrajac, D., Dodd, N., 2012. Experimental study of bore-driven swash hydrodynamics on impermeable rough slopes. Coast. Eng. 60, 149-166. http://dx.doi.org/10.1016/j.coastaleng.2011.09.006.

Lanckriet, T.M., Puleo, J.A., Masselink, G., Turner, I.L., Conley, D.C., Blenkinsopp, C., Russell, P., 2014. A Comprehensive Field Study of Swash-Zone Processes, Part 2: Sheet Flow Sediment Concentrations During Quasi-Steady Backwash. J. Waterw. Port Coast. Ocean Eng. 140, 29-42. http://dx.doi.org/10.1061/(ASCE)WW.1943-5460.0000209.

Masselink, G., Hughes, M., 1998. Field investigation of sediment transport in the swash zone. Cont. Shelf Res. 18, 1179-1199. http://dx.doi.org/10.1016/S0278-4343(98)00027-2.

Masselink, G., Evans, D., Hughes, M.G., Russell, P., 2005. Suspended sediment transport in the swash zone of a dissipative beach. Mar. Geol. 216, 169-189. http://dx.doi.org/10.1016/j.margeo.2005.02.017.

Masselink, G., Puleo, J.A., 2006. Swash-zone morphodynamics. Cont. Shelf Res. 26, 661-680. http://dx.doi.org/10.1016/j.csr.2006.01.015.

Masselink, G., Russell, P., Turner, I., Blenkinsopp, C., 2009. Net sediment transport and morphological change in the swash zone of a high-energy sandy beach from swash event to

tidal cycle time scales. Mar. Geol. 267, 18-35. http://dx.doi.org/10.1016/j.margeo.2009.09.003.

Nielsen, P., 2002. Shear stress and sediment transport calculations for swash zone modelling. Coast. Eng. 45, 53-60. http://dx.doi.org/10.1016/S0378-3839(01)00036-9.

O'Donoghue, T., Pokrajac, D., Hondebrink, L.J., 2010. Laboratory and numerical study of dambreak-generated swash on impermeable slopes. Coast. Eng. 57, 513-530. http://dx.doi.org/10.1016/j.coastaleng.2009.12.007.

Osborne, P.D., Rooker, G.A., 1999. Sand Re-Suspension Events in a High Energy Infragravity Swash Zone. J. Coast. Res. 15, 74-86. http://www.jstor.org/stable/4298916.

Petti, M., Longo, S., 2001. Turbulence experiments in the swash zone. Coast. Eng. 43, 1-24. http://dx.doi.org/10.1016/S0378-3839(00)00068-5.

Pope, S.B., 2000. Turbulent Flows. University Press, Cambridge, UK. pp. 771.

Puleo, J.A., Beach, R.A., Holman, R.A., Allen, J.S., 2000. Swash zone sediment suspension and transport and the importance of bore-generated turbulence. J. Geophys. Res. 105, 17021-17044. http://dx.doi.org/10.1029/2000JC900024.

Puleo, J.A., Holland, K.T., Plant, N.G., Slinn, D.N., Hanes, D.M., 2003. Fluid acceleration effects on suspended sediment transport in the swash zone. J. Geophys. Res. 108, C03350. http://dx.doi.org/10.1029/2003JC001943.

Puleo, J.A., Farhadzadeh, A., Kobayashi, N., 2007. Numerical simulation of swash zone fluid accelerations. J. Geophys. Res. 112, C07007. http://dx.doi.org/10.1029/2006JC004084.

Puleo, J.A., 2009. Tidal Variability of Swash-Zone Sediment Suspension and Transport. J. Coast. Res. 25, 937-948. http://dx.doi.org/10.2112/08-1031.1.

Puleo, J.A., Lanckriet, T., Wang, P., 2012. Near bed cross-shore velocity profiles, bed shear stress and friction on the foreshore of a microtidal beach. Coast. Eng. 68, 6-16. http://dx.doi.org/10.1016/j.coastaleng.2012.04.007.

Puleo, J.A., Lanckriet, T., Blenkinsopp, C., 2014a. Bed level fluctuations in the inner surf and swash zone of a dissipative beach. Mar. Geol. 349, 99-112. http://dx.doi.org/10.1016/j.margeo.2014.01.006.

Puleo, J.A., Blenkinsopp, C., Conley, D.C., Masselink, G., Turner, I.L., Russell, P., Buscombe, D., Howe, D., Lanckriet, T.M., McCall, R.T., Poate, T., 2014b. A Comprehensive Field Study of Swash-Zone Processes, Part 1: Experimental Design with Examples of Hydrodynamic and Sediment Transport Measurements. J. Waterw. Port Coast. Ocean Eng. 140, 14-28. http://dx.doi.org/10.1061/(ASCE)WW.1943-5460.0000209.

Raubenheimer, B., Elgar, S., Guza, R.T., 2004. Observations of swash zone velocities: A note on friction coefficients. J. Geophys. Res. 109, C01027. http://dx.doi.org/10.1029/2003JC001877.

Swart, D.H., 1974. Offshore sediment transport and equilibrium beach profiles. Laboratory Publication No. 131, Delft Hydraulics.

Turner, I.L., Russell, P.E., Butt, T., 2008. Measurement of wave-by-wave bed-levels in the swash zone. Coast. Eng. 55, 1237-1242. http://dx.doi.org/10.1016/j.coastaleng.2008.09.009.

Wei, T., Willmarth, W.W., 1989. Reynolds-number effects on the structure of a turbulent channel flow. J. Fluid Mech. 204, 57-95.

Figure captions and sizing

Figure 1 – single column

Fig. 1. Location of Perranporth Beach, UK (modified from Masselink *et al*., 2005), showing the location of the instrument rig.

Figure 2 – single column

Fig. 2. Offshore wave conditions on 12 and 13 October 2011, measured by a Datawell Directional Waverider buoy in approximately 10 m water depth. (A) Significant wave height H_s, (B) spectral peak period T_p, and (C) wave direction θ. Horizontal dashed line in (C) is shore normal incidence. The shaded regions in all plots indicate the two high tide sampling periods.

Figure 3 – 1.5 column

Fig. 3. Beach profile measured prior to the high tide sampling period on 12 October 2011 (A). Elevation is relative to Ordnance Datum Newlyn (ODN). The horizontal dashed line represents the mean high water (MHW) level. The thick black lines indicate the position of the scaffold rig with the main instrument bar identified by the black square. Images of the scaffold rig (B) and the three Vectrino II sensors (C).

Figure 4 – single column

Fig. 4. Five minutes of raw data collected by the bed level sensor on the main instrument bar during the sampling period on 12 October 2011.

Figure 5 – 1.5 column

Fig. 5. Time series of swash depth (A,B) and cross-shore flow velocity at multiple elevations above the bed (C,D) for the individual swash event (left panels) and ensemble swash event (right panels). Positive velocities are onshore-directed (uprush) and negative velocities are offshore-directed (backwash). Vertical dashed lines indicate the time of flow reversal. Dashed lines in (B) indicate variability of the ensemble swash event.

Figure 6 – full page width

Fig. 6. Cross-shore velocity profile (A,E), the logarithmic model estimate of the velocity profile (B,F), percent error between the measured data and the logarithmic model estimate (C,G) and correlation coefficient (r^2) for the logarithmic model fit (D,H) for the individual swash event (left panels) and the ensemble swash event (right panels). Positive velocities are onshore-directed (uprush) and negative velocities are offshore-directed (backwash). The shaded areas in (D,H) are the 95% confidence limits on the correlation coefficients. The dashed line in (D,H) indicates the r^2 cut-off (0.8 for the individual event, 0.9 for the ensemble event) below which model fit is deemed poor and data are removed from (B,C,F,G). Vertical dashed lines indicate the time of flow reversal. Note the scale change between the individual and ensemble swash events.

Figure 7 – full page width

Fig. 7. Cross-shore velocity profiles (C,D) extracted from 8 evenly spaced times during the individual swash event (left panels) and ensemble swash event (right panels), and corresponding time series from the uppermost bin of each event (A,B). Positive velocities are onshore-directed (uprush) and negative velocities are offshore-directed (backwash). The locations of the coloured profiles in (C,D) correspond to the coloured dots in (A,B). Solid curves are logarithmic model fits if r^2 > 0.8 or 0.9 for the individual and ensemble swash

events respectively. The vertical dashed line in (A,B) indicates the time of flow reversal. Horizontal dashed lines in (C) distinguish the profiling range of the three Vectrino II sensors. Note the scale change between the individual and ensemble swash events.

Figure 8 – 1.5 column

Fig. 8. Bed shear stress τ estimated from the logarithmic model and the quadratic drag law (A,B) and friction coefficients f (C,D) for the individual swash event (left panels) and ensemble swash event (right panels). The quadratic drag law (Eq. (3)) was used with a constant f value of 0.012 based on the Swart (1974) formula (horizontal dashed line in (C,D)) and u_f from 0.07 m and 0.02 m for the individual and ensemble swash events respectively. Vertical dashed lines indicate the time of flow reversal.

Figure 9 – single column

Fig. 9. Bed shear stress τ estimated from the logarithmic model fit to different maximum elevations in the velocity profile for the individual swash event (A) and ensemble swash event (B). Vertical dashed lines indicate the time of flow reversal.

Figure 1

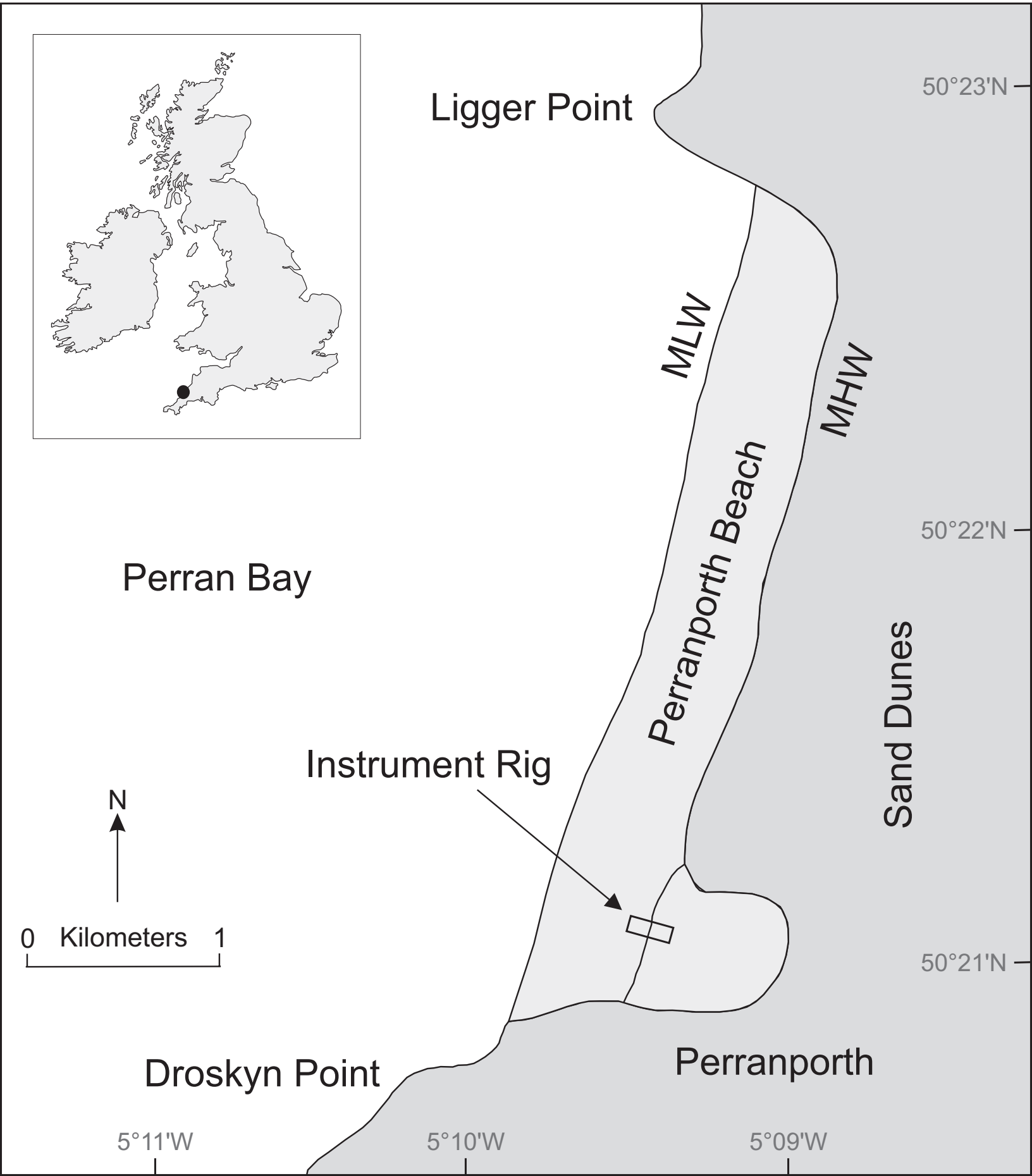
Ligger Point
50°23'N
MLW
MHW
Perranporth Beach
Sand Dunes
50°22'N
Perran Bay
Instrument Rig
N
0 Kilometers 1
50°21'N
Droskyn Point
Perranporth
5°11'W
5°10'W
5°09'W

Figure 2

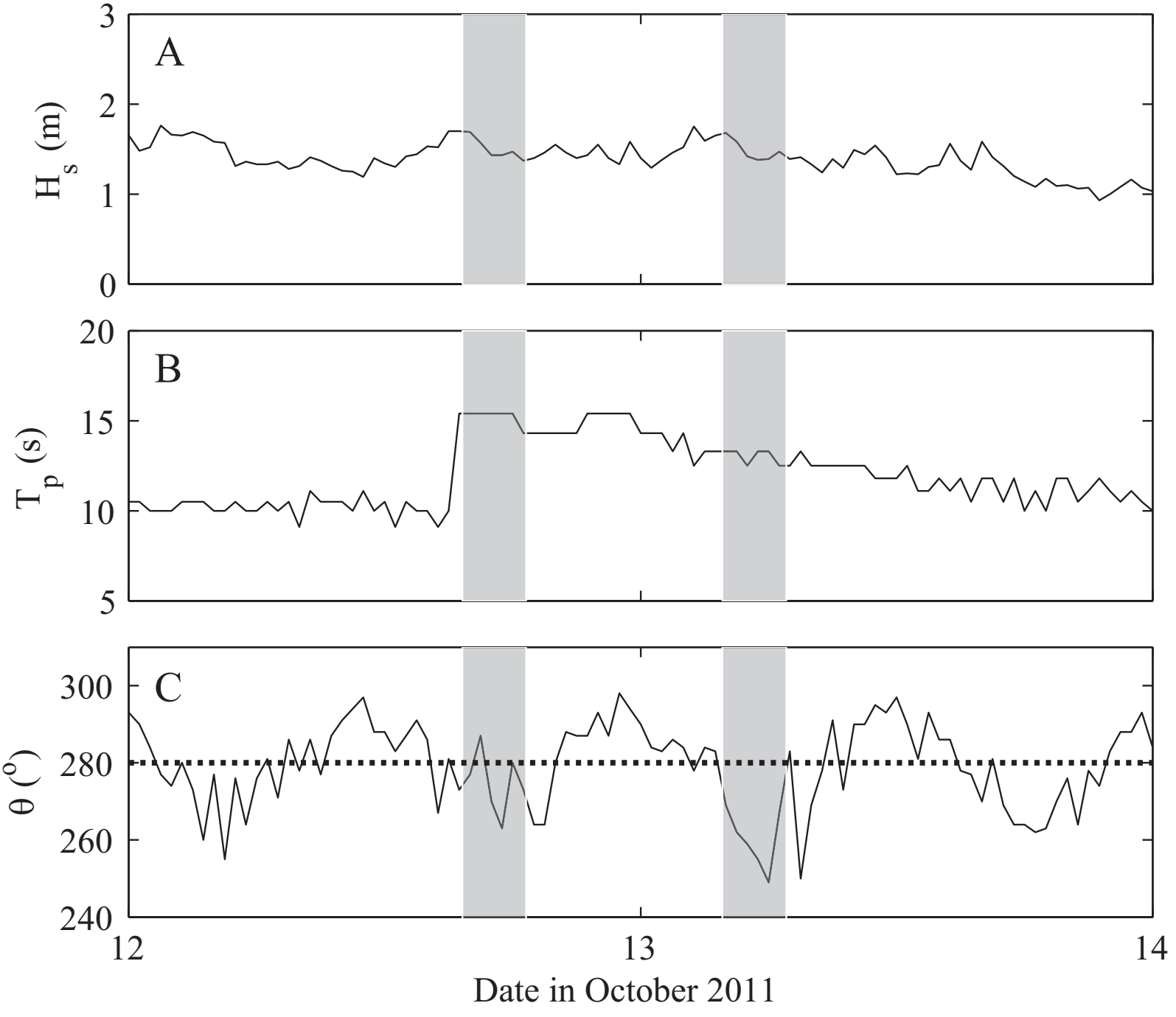
A
B
C
H_s (m)
T_p (s)
θ (°)
3
2
1
0
20
15
10
5
300
280
260
240
12
13
14
Date in October 2011

Figure 3

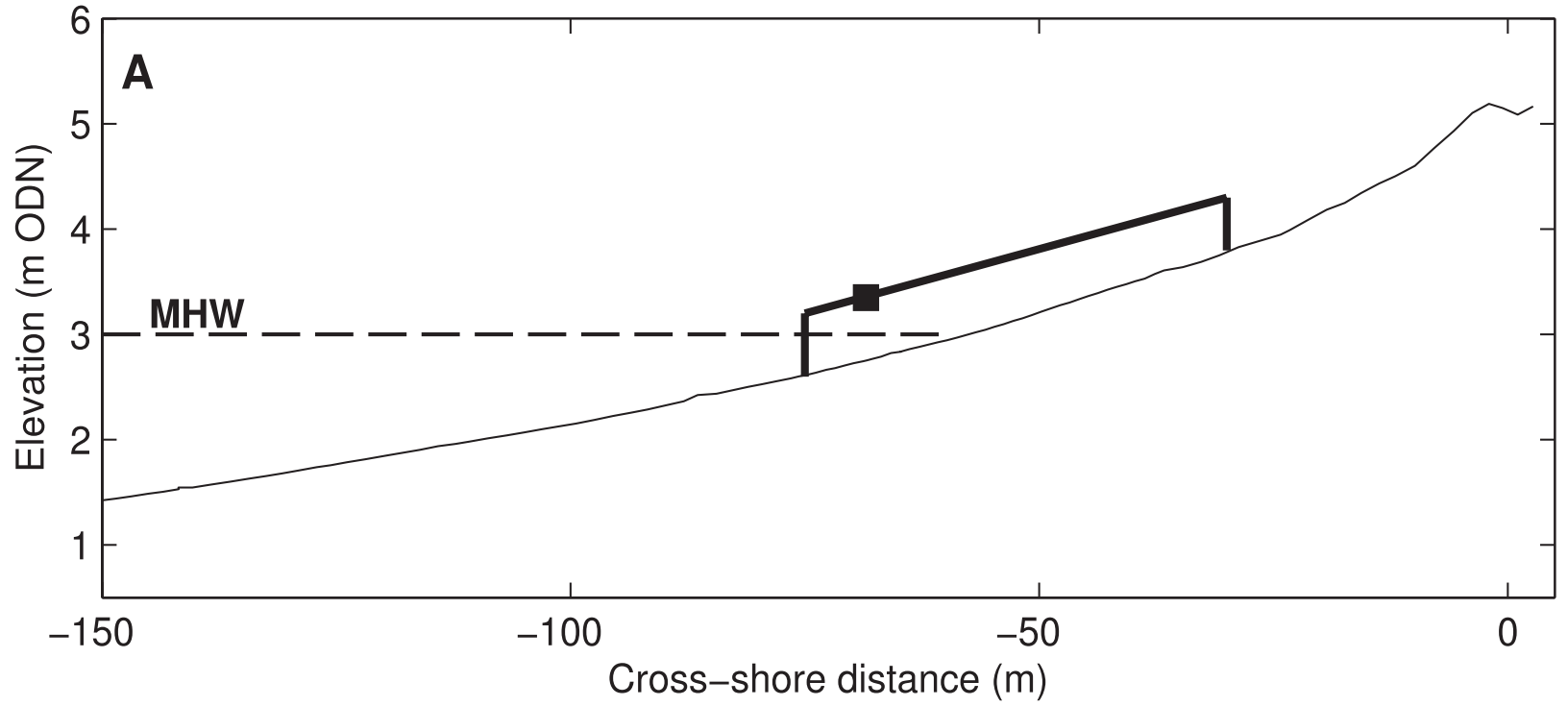
A
MHW
Elevation (m ODN)
6
5
4
3
2
1
−150
−100
−50
0
Cross−shore distance (m)

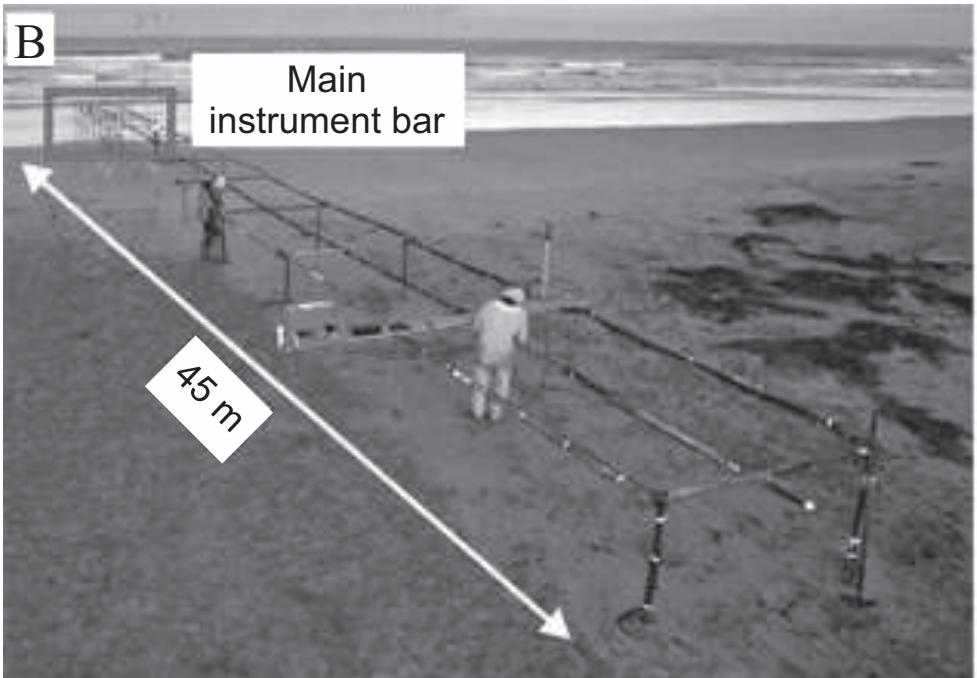
B
Main
instrument bar
45 m

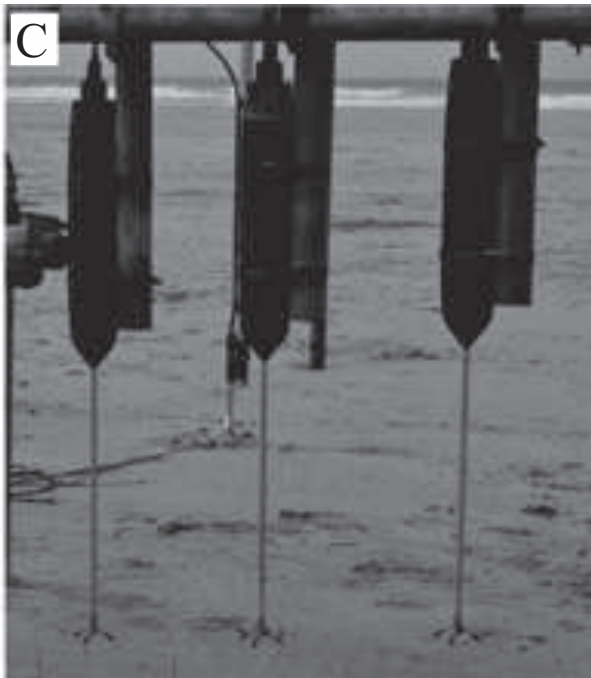
C

Figure 4

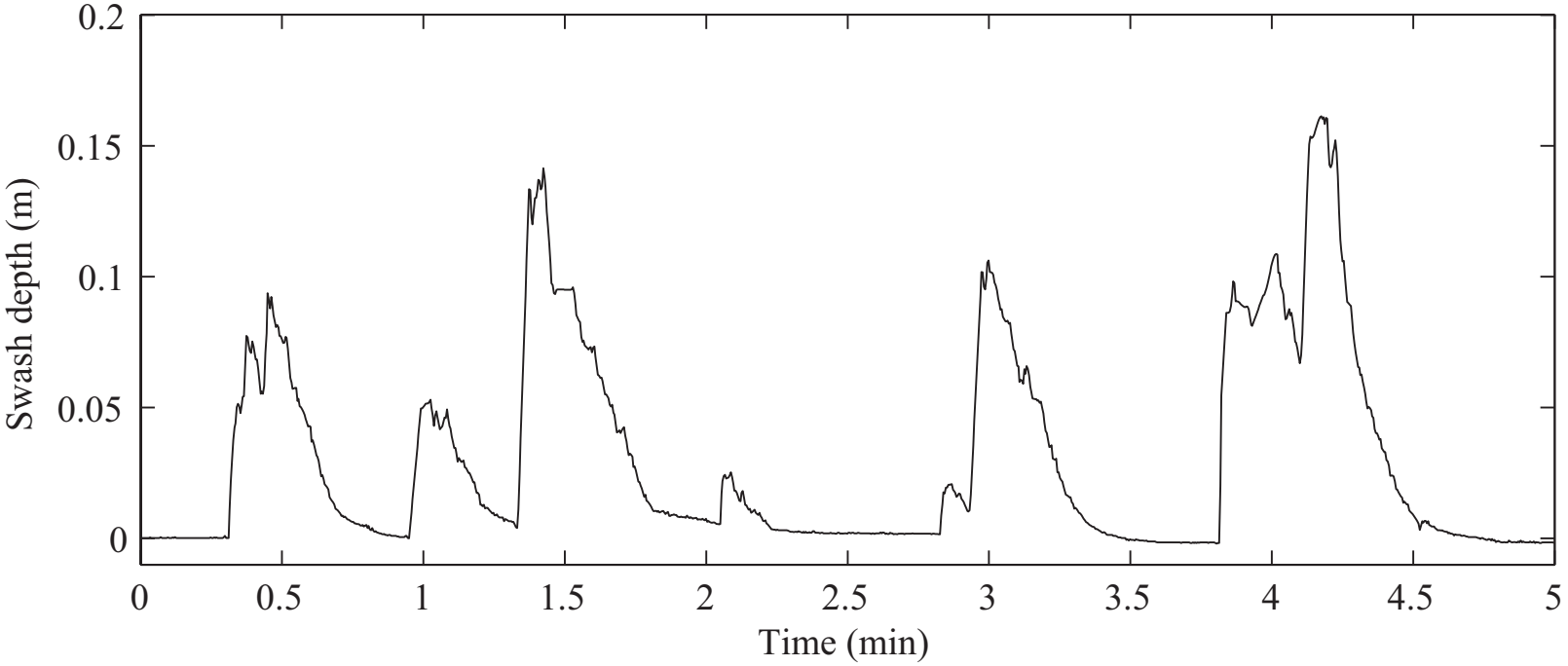

Figure 5

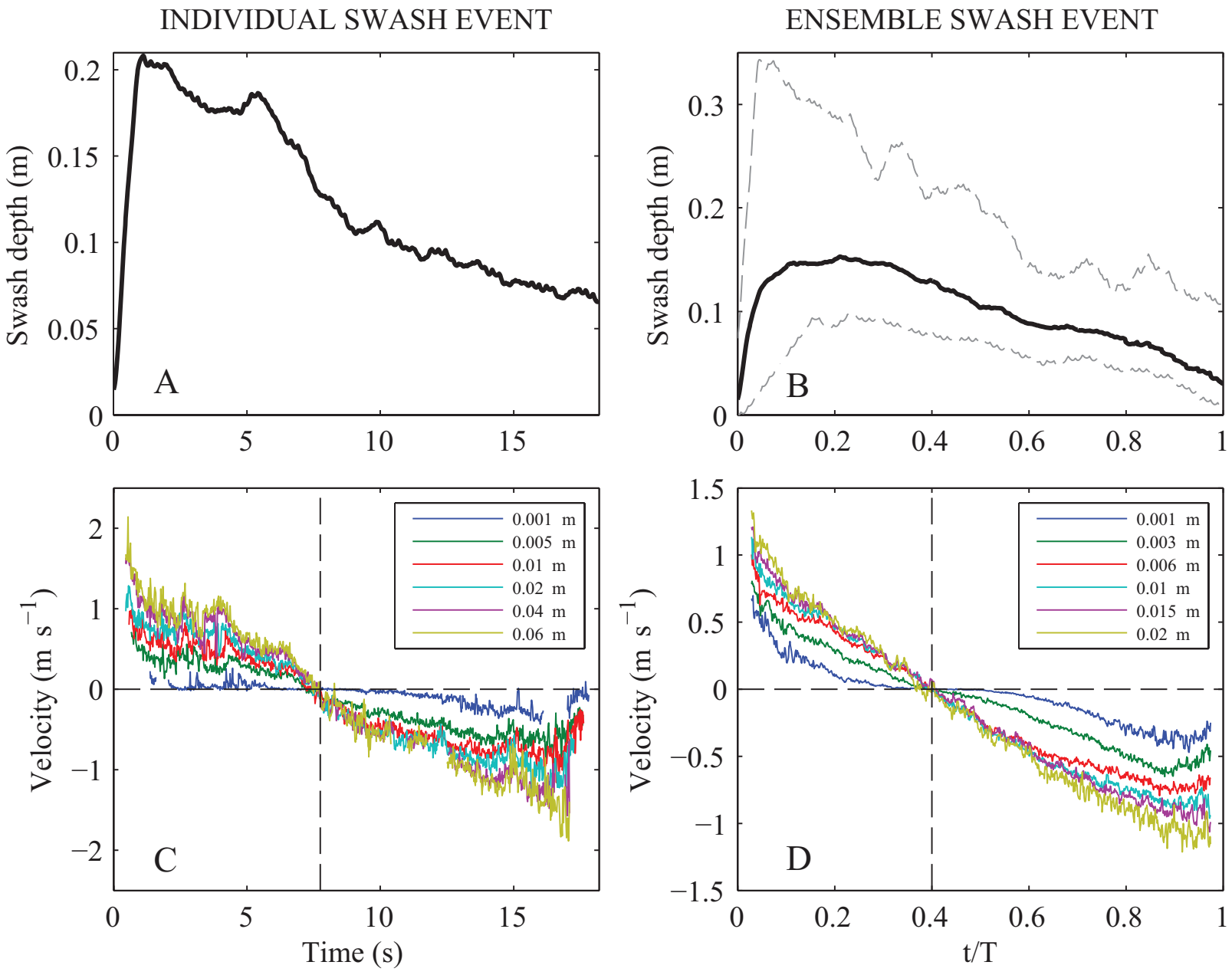
INDIVIDUAL SWASH EVENT
ENSEMBLE SWASH EVENT
Swash depth (m)
A
B
C
D
Velocity (m s^{-1})
Time (s)
t/T
0.001 m
0.005 m
0.01 m
0.02 m
0.04 m
0.06 m
0.003 m
0.006 m
0.015 m

Figure 5 bw

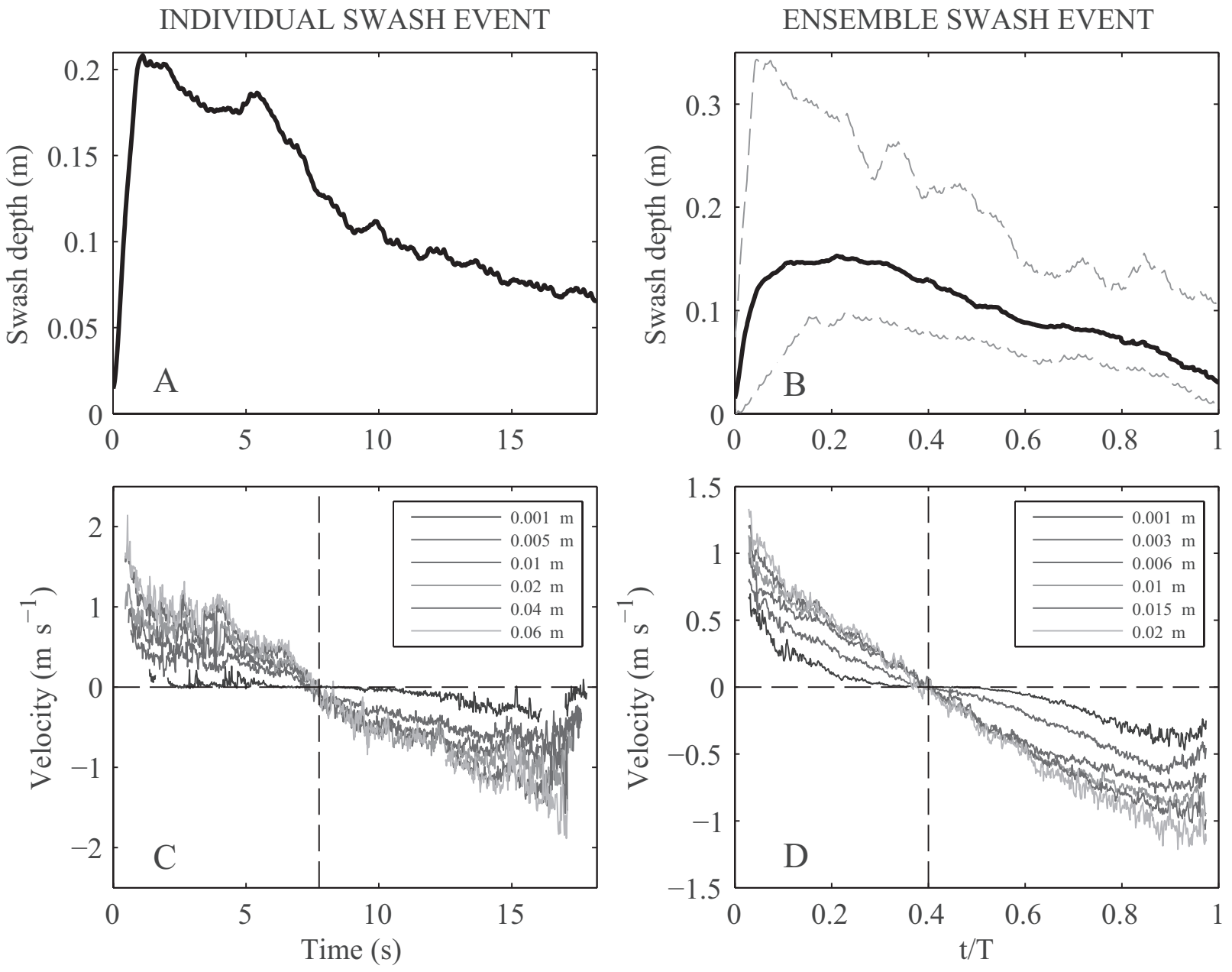
INDIVIDUAL SWASH EVENT
ENSEMBLE SWASH EVENT
Swash depth (m)
A
B
C
D
Velocity (m s^{-1})
Time (s)
t/T
0.001 m
0.005 m
0.01 m
0.02 m
0.04 m
0.06 m
0.003 m
0.006 m
0.015 m

Figure 6

Click here to download high resolution image

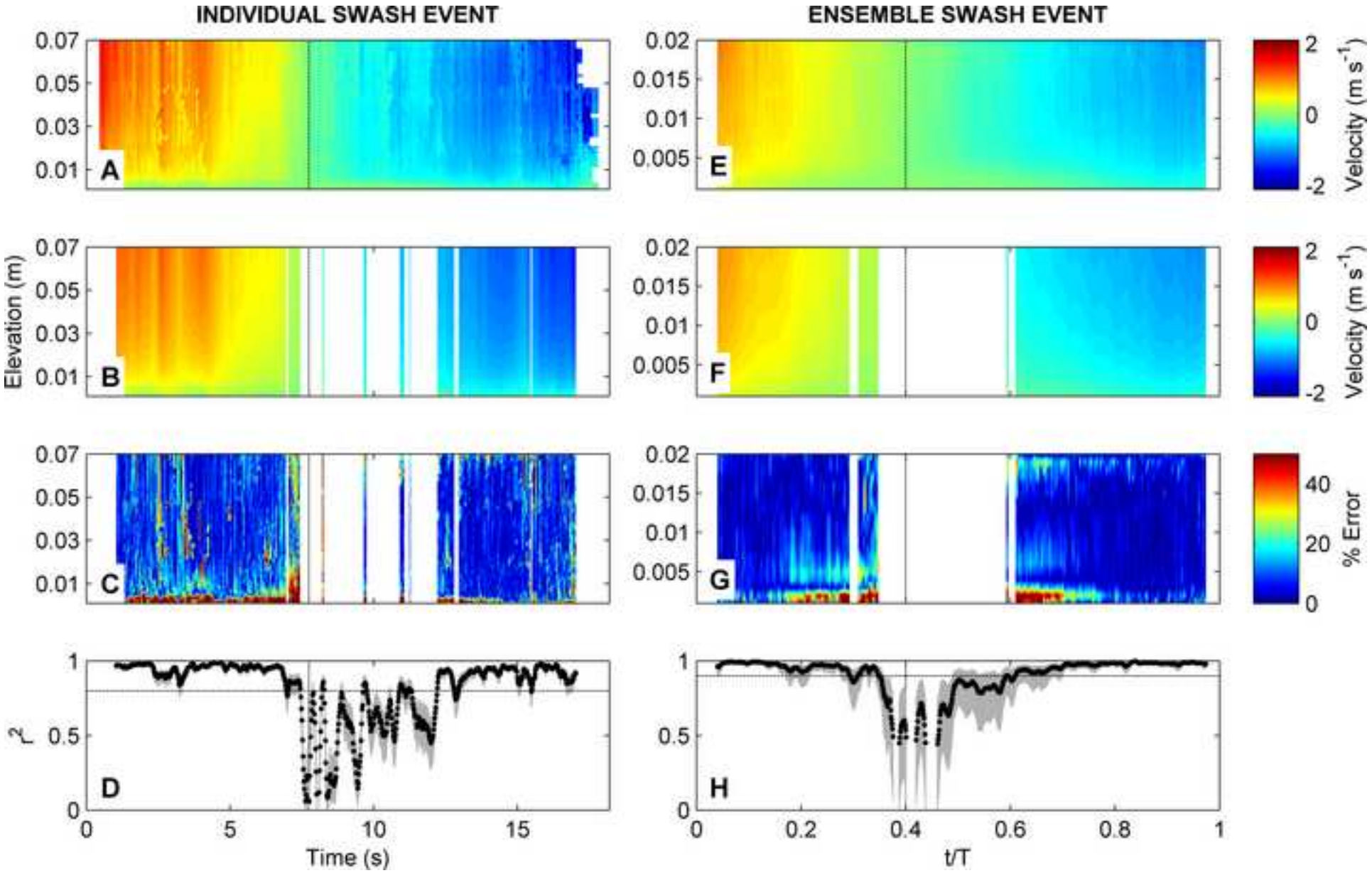

Figure 6 bw

Click here to download high resolution image

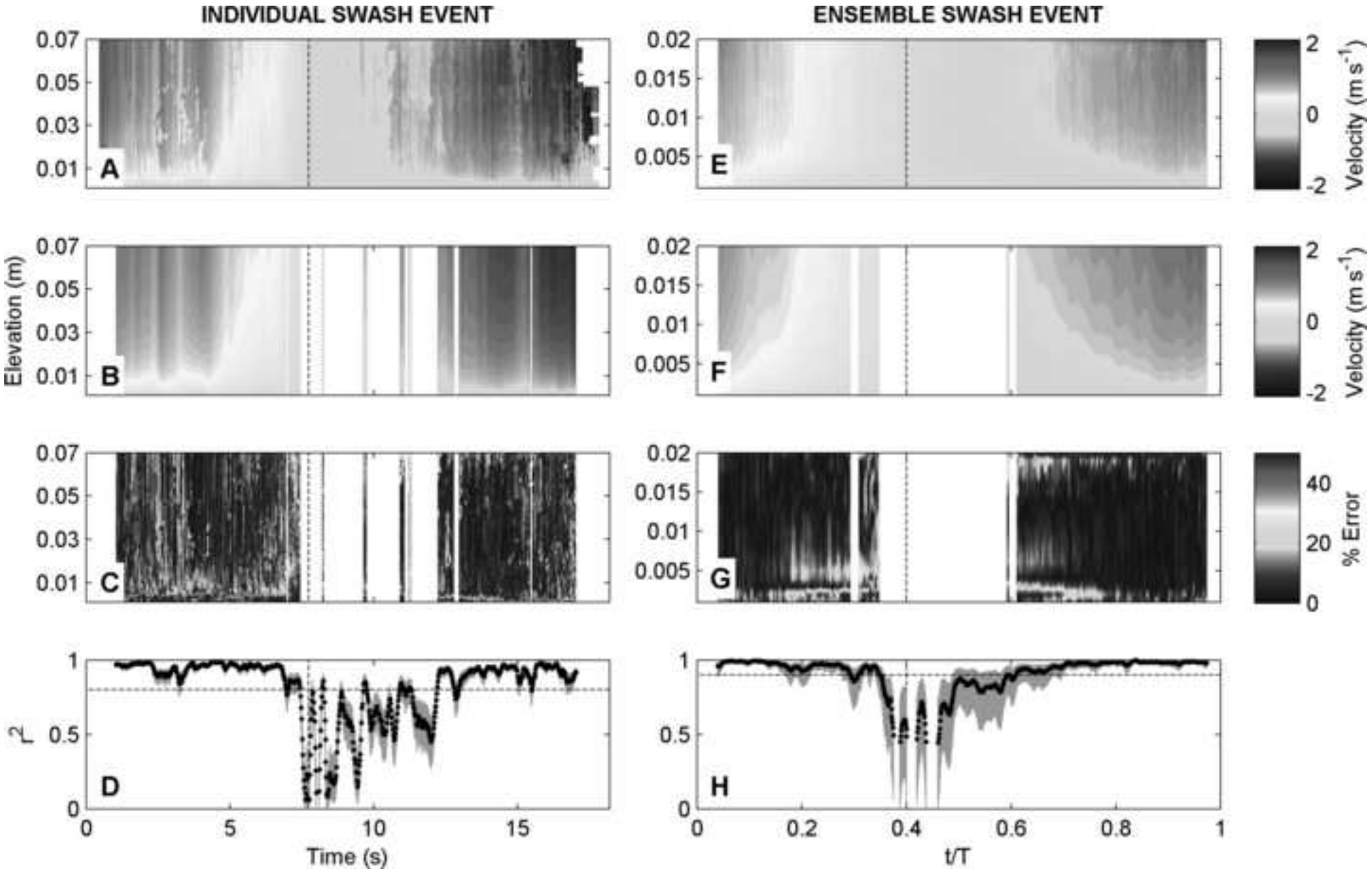

Figure 7

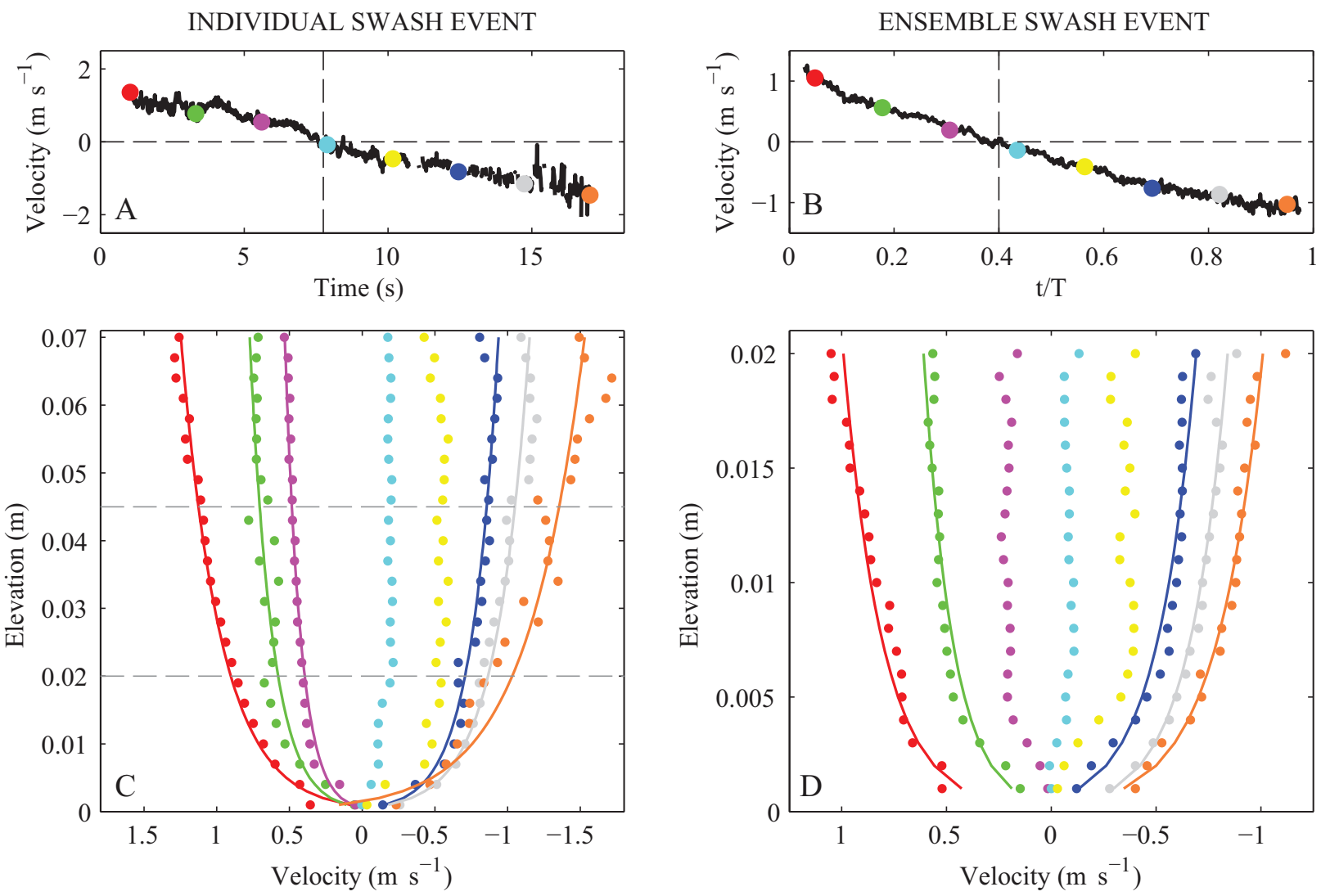
INDIVIDUAL SWASH EVENT
ENSEMBLE SWASH EVENT
Velocity (m s^{-1})
Time (s)
t/T
A
B
C
D
Elevation (m)
Velocity (m s^{-1})

Figure 7 bw

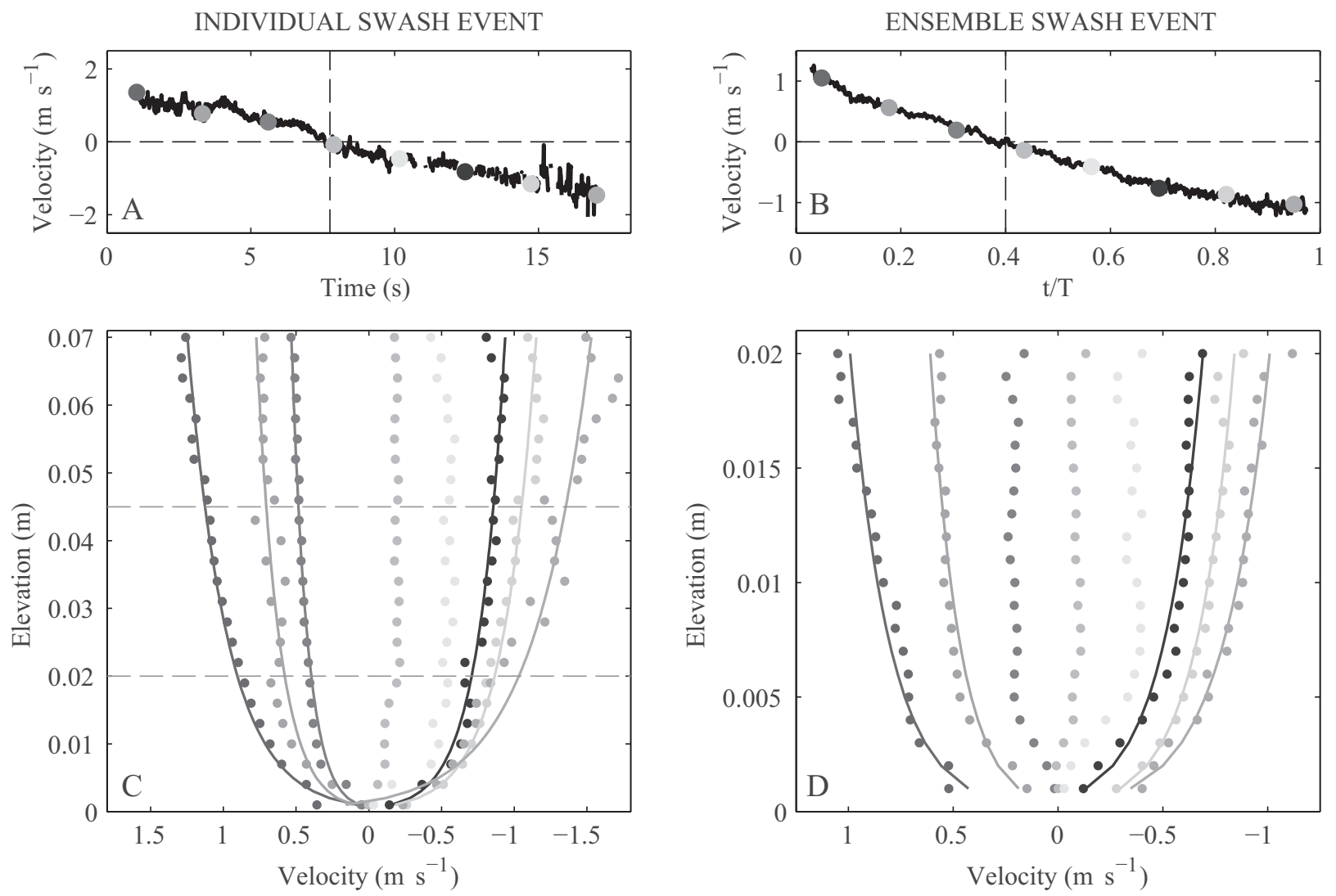
INDIVIDUAL SWASH EVENT
ENSEMBLE SWASH EVENT
Velocity (m s^{-1})
A
B
Time (s)
t/T
Elevation (m)
C
D
Velocity (m s^{-1})

Figure 8

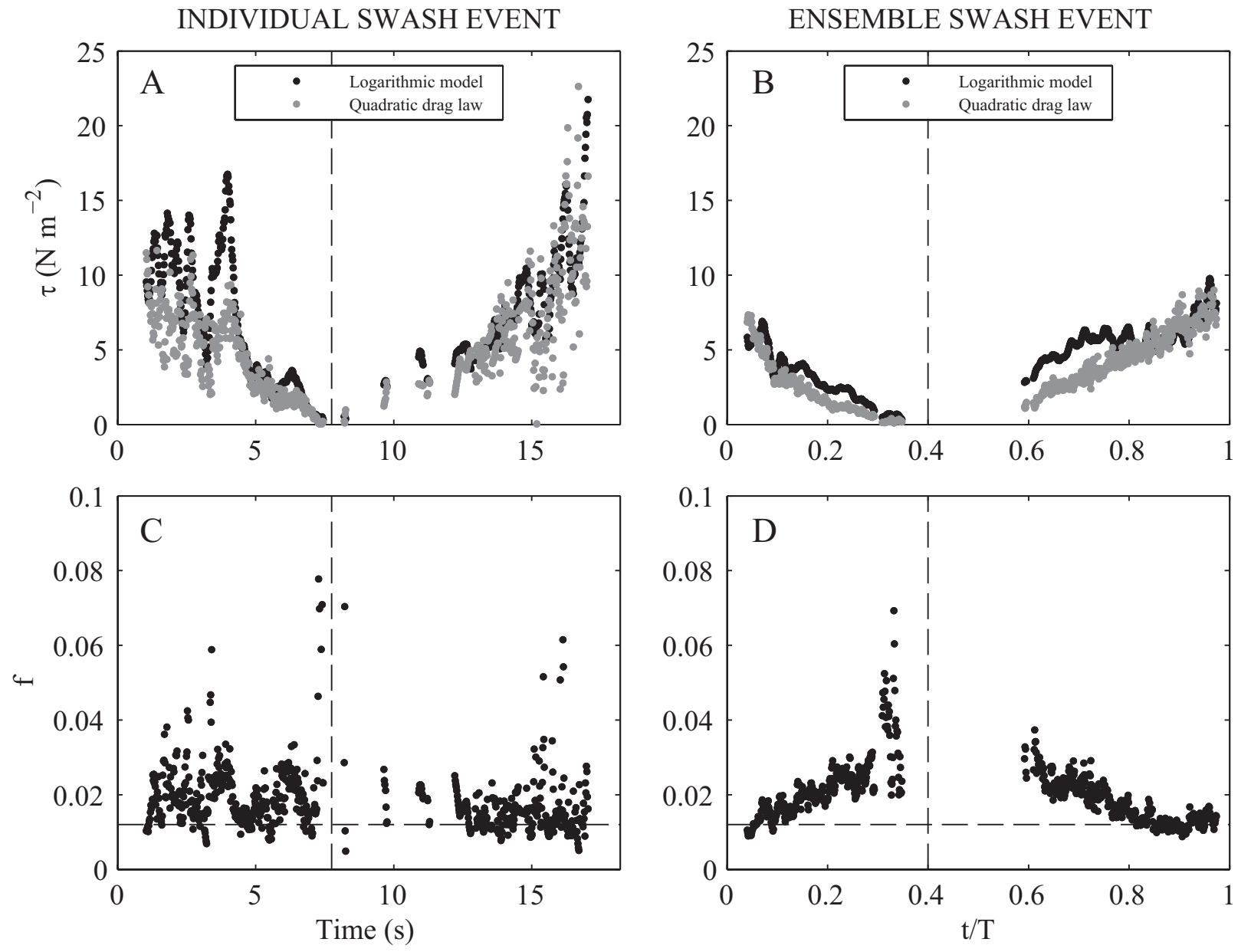
INDIVIDUAL SWASH EVENT
ENSEMBLE SWASH EVENT
A
B
C
D
Logarithmic model
Quadratic drag law
τ (N m^{-2})
f
Time (s)
t/T

Figure 9

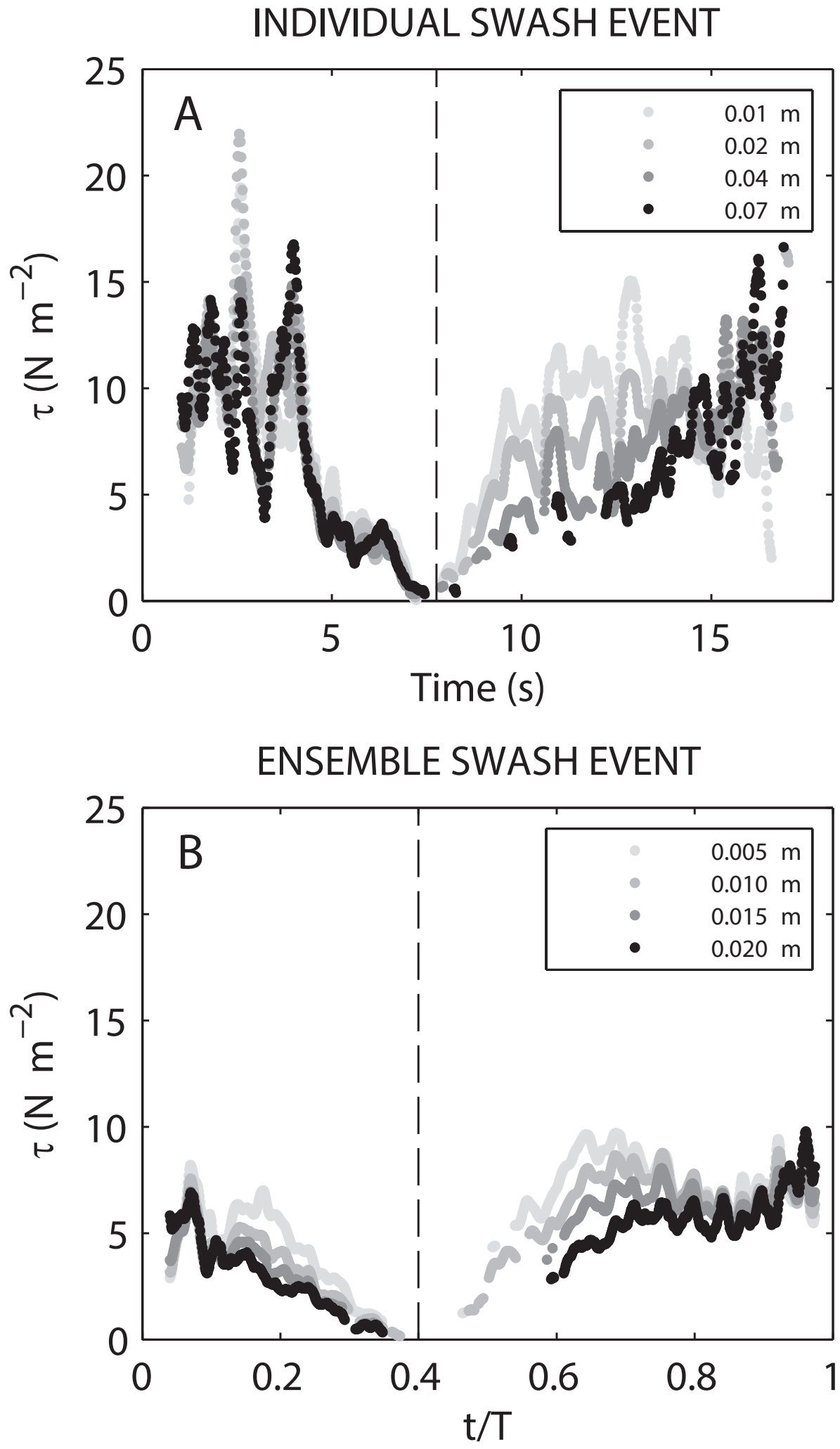
INDIVIDUAL SWASH EVENT
A
0.01 m
0.02 m
0.04 m
0.07 m
τ (N m−2)
Time (s)
ENSEMBLE SWASH EVENT
B
0.005 m
0.010 m
0.015 m
0.020 m
τ (N m−2)
t/T